Electric Power Systems Research 201 (2021) 107504

Contents lists available at ScienceDirect

Electric Power Systems Research

journal homepage: www.elsevier.com/locate/epsr

Transmission line protection algorithm based on voltage sequence component under high penetration of inverter-based resources

Safa Kareem Al-sachit [1,*], Nirmal K.C Nair

Department of Electrical, Computer and Software Engineering, University of Auckland, 3 Grafton Road, Auckland 1010, New Zealand

ARTICLE INFO

Keywords:
Fault detection
Fault voltage sequence components
Inverter-based resources
Transmission line protection
Wind turbine generator
Weak infeed source

ABSTRACT

A new protection algorithm based on sequence voltage components is proposed in this paper. The new algorithm helps overcome the sensitivity and maloperation issues of the traditional protection schemes in the transmission line network, especially with a high penetration level of inverter-based resources. In this algorithm, the differential fault sequence components are used to identify faulty events in the transmission network. The fault voltage component across the protected line is compared to a setting value of multiple parameters-based voltage makes the final decision of tripping for internal faults only. The proposed algorithm has been tested on a 400kV, 50 Hz single circuit transmission line network supplied with a mix of 90% wind turbines and 10% synchronous generators. The new algorithm simulation testing showed high accuracy when it comes to rapid trip activation with high discrimination reliability between internal and external events. High impedance with different fault locations has been tested to improve the proposed algorithm reliability. The study also performed on the IEEE 9-bus system to validate the proposed algorithm under various faults when strong and weak infeed performed into a bigger transmission network.

1. Introduction

The increasing concerns about climate change result in expecting an enormous increment of renewable energy resources in the generation, transmission, and distribution side of the power network. These renewables are usually connected to the network through power electronics, e.g., inverters; hence it denoted as inverter-based resources (IBRs). Although inverters have been designed to have flexible control during the steady-state condition, it has arisen new challenges for the power system during abnormal events led to skepticism in the existing protection system reliability [1][2]. These challenges emerged from the different responses of IBRs to faulty events comparing to the existing synchronous generators, particularly on transmission protection systems. These impacts include the small fault current contribution from IBRs comparing to the traditional synchronous generator. The control schemes used with renewable resources were designed to allow only a limited amount of fault current to pass to avoid the thermal damage of their switching elements and the DC bus capacitor. This behavior results in the following:

1 Providing a large negative sequence impedance during the faulty event and a very low or negligible amount of negative and zero sequence current components required by protection relays to guarantee high performance of fault detection. However, the amount of injected negative sequence current is highly dependent on the IBRs' type and their control scheme.
2 Short transient duration response. The IBRs are not responding immediately, taking more than one cycle according to [3], which is more than the time required by protection relays to trip. In other words, these resources' injection of the negative sequence current is not controlled.
3 Changes in angular relation of current and voltage phasors depending on the faulty section's needs, such as being under ride through requirement or reactive support requirements. Hence, it suppressed the sequence components required for reliable fault identification [4].
4 The inconsistent response between inverters of one manufacturer to another manufacturer. As some manufactures allow negative sequence current injection of some amount and others are not. Hence, resulting in uncontrolled phase angle between negative

* Corresponding author.
[1] *E-mail address*: sals931@aucklanduni.ac.nz (S. Kareem Al-sachit)

https://doi.org/10.1016/j.epsr.2021.107504
Received 11 April 2021; Received in revised form 23 July 2021; Accepted 4 August 2021
Available online 16 August 2021

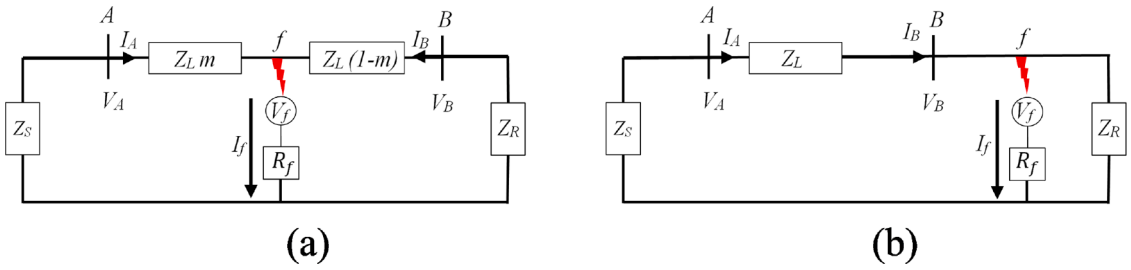

Fig. 1. Simple fault component distribution of two-terminal transmission system network (a) Internal fault, (b) External fault

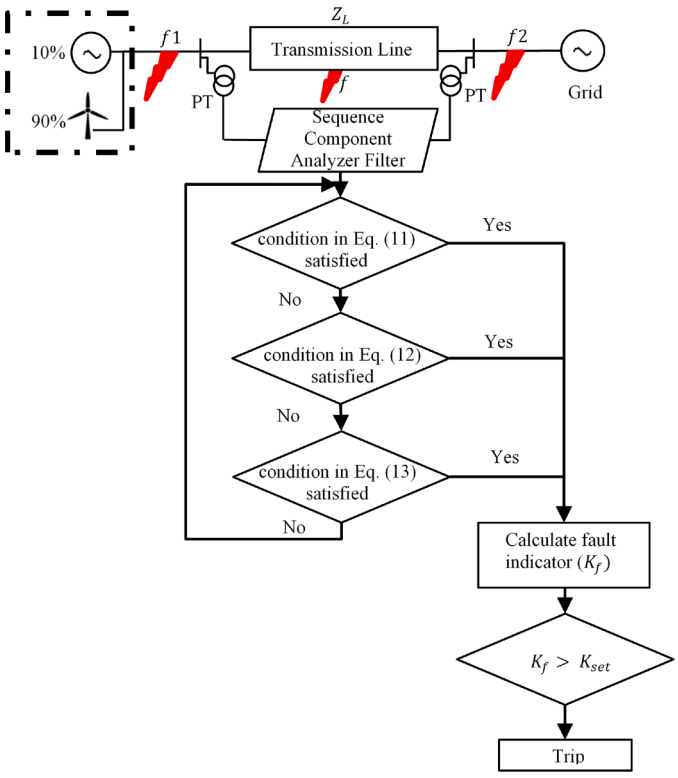

Fig. 2. Fault tripping procedure of the proposed algorithm

sequence components of voltage and current, especially with the absence of standards widely.

Moreover, the type of renewable resource, location, the availability of renewable energy, generation capacity and the different short circuit characteristics would also challenge transmission systems protection reliability. Based on the aforementioned challenges alongside the fault type and location, Transmission Lines ' (TL) distance protection schemes might over/under reach due to the oscillation of the apparent impedance depending on the injected amount of current from the connected IBR. Hence, the distance relays zone setting would be affected and miscoordinating up-stream and downstream relays[5]. Test results in [6] showed that distance relay might mal-operate for out of zone fault events or might not trip for internal, in-zone ones. [7] showed that under intermediate to high integration levels of IBRs and according to the control strategy, distance relay might oppose any applied fault ride through criteria due to relay's overreaching.

[3] discussed the impact of IBR current injection on TL distance protection, showing how distance relay may overreach or even drop out due to apparent impedance oscillation based on injected negative sequence current. However, the latter study showed that differential protection is a reliable scheme despite its high requirements in terms of cost, communication, response to high impedance earth faults, two-phase operation of TL and need for backups. Nevertheless, there still not enough studies on differential protection performance when IBRs are the predominant power supply.

Phase comparison protection schemes maloperation has been tested in [8]. The study showed how the relay's sensitivity reduced due to the negative sequence current phase angle shifting during faulty events as the relay considered this phase difference as an external fault and not to trip on it.

As a result, maintaining reliability has become more complicated, and transmission operators have been looking at other possibilities to ensure a secure and dependable power system. Some of these solutions might involve modifying or upgrading protection relays settings [9, 10] or replacing existing relays with newer and more flexible technologies adaptable to relays' application guides and standards [11, 12].

In the last few decades, a new direction of using voltage-based relay has come under study. There were proposals in detecting faults under high IBRs penetration in low/medium voltage distribution networks. The study in [13] is based on converting the measured voltage to the dq frame. [14] proposed an adaptive voltage scheme based on the relationship between pre and post-fault phase voltage difference. Similarly, for wide-area protection [15] proposed using fault voltage components to identify faulty buses using the ratio of the measured bus voltage to its calculated value as fault detection element.

For a high voltage transmission network under high penetration of IBR on the generation side, a similar concept can be adopted to avoid the challenges associated with these resources and their power electronic interface components. In this context, this paper intends to propose a new TL protection algorithm based on differential fault voltage sequence components as a fault identification element where less dependency on low fault current and its negative sequence component supplied from IBRs is applied. The main contribution of this paper based on developing a new fault identification index that uses the fault measured drop voltage sequence components across the protected line and compare it to a setting value of multiple parameters making the final decision of tripping for internal faults only. The automatically determined threshold value makes the proposed algorithm unique, flexible, and adaptable to different fault events. The proposed algorithm can identify different fault types accurately with high sensitivity discriminating internal and external events.

The rest of the paper is organized as follows; Section II discusses the new scheme in detail; the type IV full-scale converter wind power plant is considered in this paper as an example of IBRs. Section III involves the hardware implementation of the proposed protection relay. Section IV presents the simulation result and discusses the new protection algorithm reliability with a bigger network under the presence of a weak infeed source. Section V concludes the proposed algorithm features.

2. Fault voltage component base protection algorithm

The proposed algorithm aims to identify all fault types occurrence and distinguish the internal events from the external ones. In this algorithm, current and voltage sequence components have been utilized.

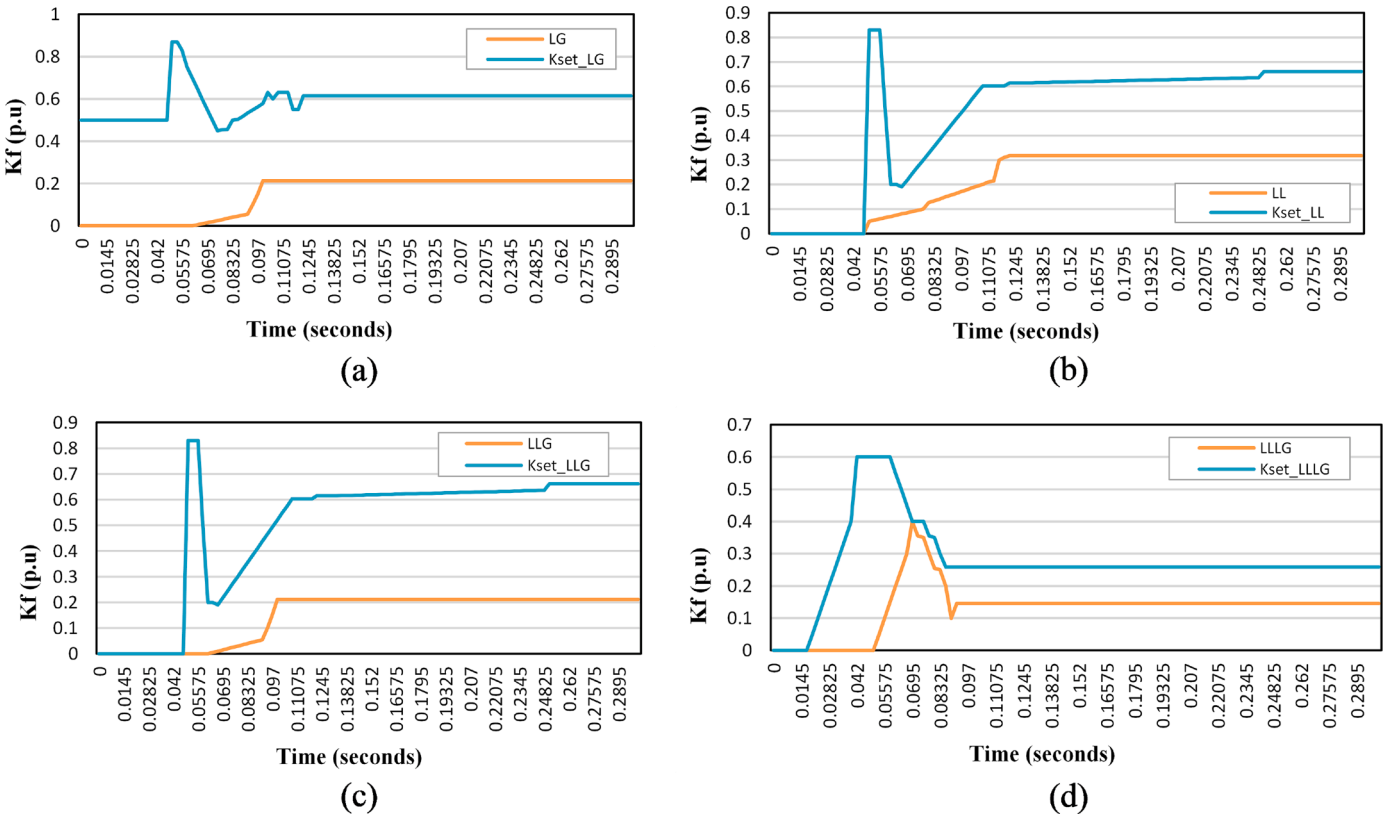

Fig. 3. Fault indicator and setting behaviour during External fault near bus A: (a) SLG fault, (b) LL fault, (c) LLG fault, (d) LLLG fault.

2.1. Basic principle and setting

The principle of the proposed algorithm is based on estimating the voltage sequence component difference at each side of the protected line. The voltage across the protected line impedance remains unchanged during the normal operating condition and as well as during external fault events, as shown in Fig.1(b) where the voltage across the line according to Kirchhoff's current law as follows:

$$I_A = I_B \tag{1}$$

$$V_A - V_B = I_A Z_L \tag{2}$$

The ratio of the difference between voltages at both ends of the protected line to their summing when the system operates normally or during external fault will be low compared to the setting value. The voltage across the line impedance will always equal the line's local/remote side voltage depending on the external event position. However, those voltages are never the same when a fault occurs within the protected section of the line. This principle has been used to estimate the fault indicator (K_f) of the proposed algorithm.

By applying Kirchhoff's voltage law on Fig.1(a), the voltage across the line section analyzed from the line's local end at (A) to the fault point (*f*) and from the remote end (B) to the fault point as below

$$V_A - I_A Z_L m - V_f = 0 \tag{3}$$

Similarly,

$$V_B - I_B Z_L (1-m) - V_f = 0 \tag{4}$$

By summing and subtracting (3) and (4)

$$V_A - V_B = I_A Z_L m - I_B Z_L (1-m) \tag{5}$$

$$V_A + V_B = I_B Z_L (1-m) - I_A Z_L m - 2V_f \tag{6}$$

K_f can be formulated as in (7).

$$K_f = \frac{|V_A - V_B|}{0.5(V_A + V_B)} \tag{7}$$

Where V_A and V_B are the measured voltage at buses A and B respectively with I_A and I_B are representing the measured current at buses A and B respectively. (Z_L)denotes the protected line impedance. (m) represents the distance ratio from side (A) of the line to the fault point. (V_f) is the fault voltage component at the fault point.

To estimate the algorithm setting value (K_{set}), the criterion for detection of fault is as fellow

$$K_f > K_{set} \tag{8}$$

$$K_{set} = K_{reliability} V_{rated} V_m \tag{9}$$

where $K_{reliability}$ represents the reliability percentage coefficient of the algorithm, which ranges between 0.8-0.95 and chosen to be 0.8 in this paper. The reliability factor varies based on many factors including the line impedance, line length and measurement errors. V_{rated} denotes the system rated voltage and V_m is the maximum value of the measured voltage component of the line's both terminals. The variable measured V_m plays a key role in suiting the algorithm's reliable operation. The importance of the latter parameter appears when different faults applied to the protected line. Each fault type is expected to have different voltage values that can be ranged from rated voltage magnitude for the positive sequence component to a low value for the zero sequence component. To guarantee a reliable operation of the proposed algorithm V_m has been included in the setting value calculation.

This algorithm can be used to detect all fault types based on the fault sequence components recognition, where Eq. 9 can be applied on symmetrical and asymmetrical faults as below

$$\begin{cases} K_f^0 = \dfrac{|V_A^0 - V_B^0|}{0.5(V_A^0 + V_B^0)} \\ K_f^1 = \dfrac{|V_A^1 - V_B^1|}{0.5(V_A^1 + V_B^1)} \\ K_f^2 = \dfrac{|V_A^2 - V_B^2|}{0.5(V_A^2 + V_B^2)} \end{cases} \quad (10)$$

Where 1, 2 and 0 superscripts denoted the positive, negative and zero sequence components of fault voltage respectively. Voltage components amplitude has been tested in [16] to be the highest at the line terminals for positive sequence component and more accurate for negative and zero components at the fault point. Although positive sequence component voltage can be used to identify all fault types, the negative and zero components are used in this algorithm due to their long existence period comparing to the positive one. Low voltage sequence condition (K_{com}) plays the main role in identifying the faulted area and the fault type alongside the fault detection condition in Eq. (8).

The negative and zero sequence components criterion in Eq. (10) utilized to detect asymmetrical earth fault as shown below

$$\begin{matrix} V_A^2 \ and \ \ V_B^2 > K_{com}^- \\ V_A^0 \ and \ \ V_B^0 > K_{com}^0 \end{matrix} \quad (11)$$

Where K_{com}^- and K_{com}^0 are the minimum voltage component setting measured at the local end of the protected line, which is set to be 0.2 in this paper to identify the abnormal voltage variations from the normal voltage fluctuation. If Eq. (11) is not correct for the zero-sequence component, the negative sequence voltage component at both sides of the line is used to identify line to line fault occurrence in addition to Eq. (8) condition as follows

$$V_A^2 \ and \ \ V_B^2 > K_{com}^- \quad (12)$$

Where K_{com}^- set to be 0.2. If conditions in Eq. (11) and (12) are not satisfied, a symmetrical three-phase fault will be detected, as shown in Eq. (13) with K_{com}^+ set to be < 1 for both sides measured voltages of the line. represents the proposed algorithm fault detection procedure

$$V_A^1 \ and \ \ V_B^1 < K_{com}^+ \quad (13)$$

Fig. 2

2.2. Detection of external fault

Simulation results in Fig. 3 tested the algorithm accuracy in discriminating between internal and external events. The simulation is done under (0Ω) fault resistance near bus A at f_1 position as shown in Fig.2 at time = 0.05 second. Fig. 3 (a, b, c and d) showed that K_f stayed below the setting value for all fault types; single line to ground (LG), line to line (LL), double line to ground (LLG) and three lines to ground fault (LLLG). Simulation results also showed Eqs. (11, 12 and 13) impact on increasing the algorithm selectivity as these conditions cannot be satisfied when an external fault occurs, where, in this case, at least one side voltage of the line will always be out of these conditions.

Since this algorithm performance based on utilizing measured data from both sends of the protected section of the line, a synchronized

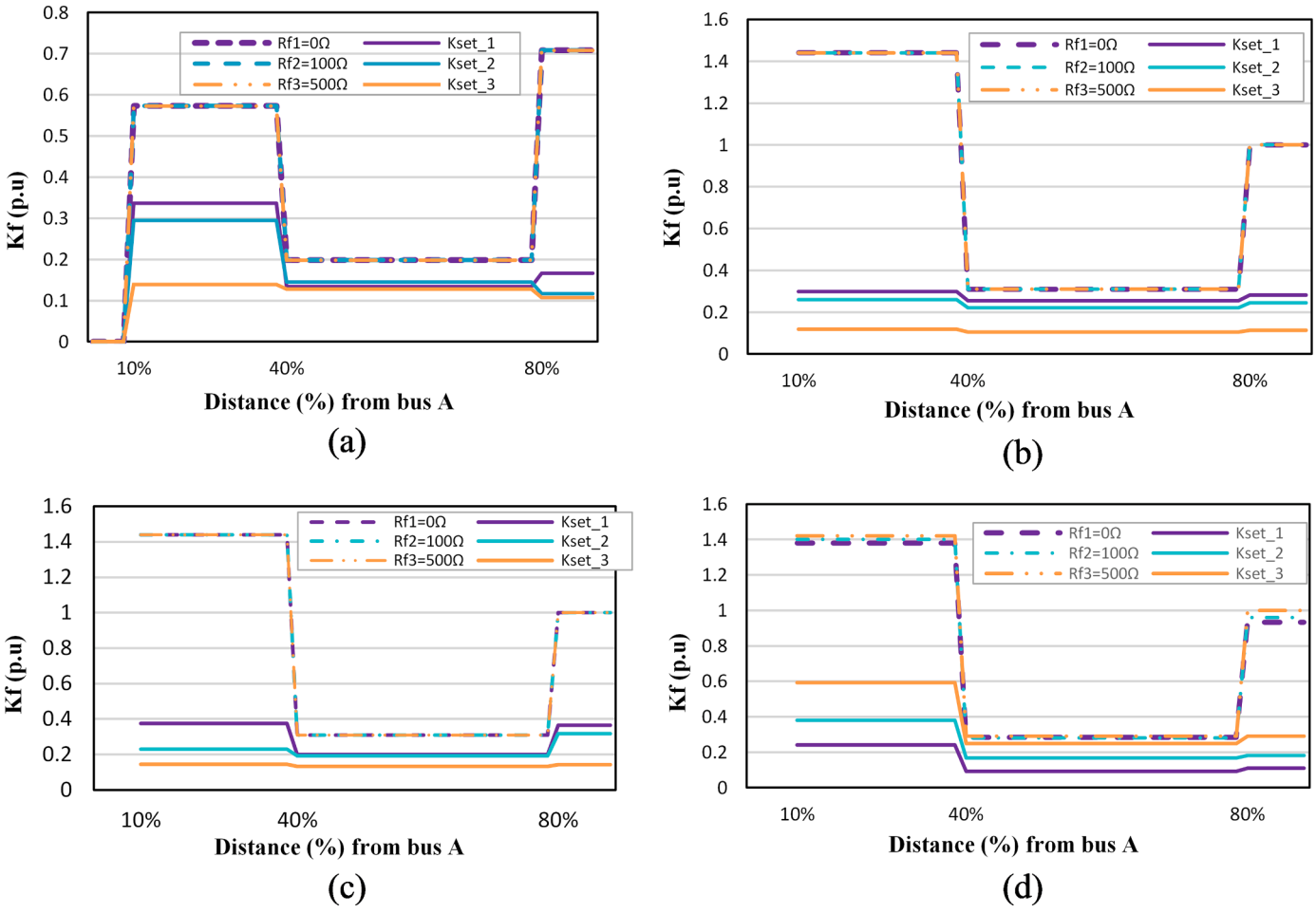

Fig. 4. Fault indicator and setting behaviour during internal (a) SLG fault, (b) LL fault, (c) LLG fault, (d) LLLG fault.

Table 1.
Voltage-Based Differential Protection Operation Under Different Fault Locations and Resistances

Fault Resistance (Ω)	Fault Position from Bus (A)	Fault Type		
		L-G	L-L	L-L-L
		Tripping/Operation Time (msec)		
0	10%	8.905	9.685	11
	40%	6.285	8.393	10.22
	80%	7.665	9.37	10.98
100	10%	12.005	11.54	12.43
	40%	8.42	10.68	11.61
	80%	10.89	11.25	12.39
500	10%	17.84	17.15	18.0
	40%	13.35	15.265	16.79
	80%	15.765	16.49	16.329

Table 2.
Voltage-Based Differential Protection Operation Under 100% Synchronous Generation

Fault Resistance (Ω)	Fault Position from Bus (A)	Fault Type		
		L-G	L-L	L-L-L
		Tripping/Operation Time (msec)		
0	10%	13.595	17.065	7.1
	40%	10.585	15.41	19.885
	80%	12.615	16.465	6.92
100	10%	15.4	20.48	8.175
	40%	12.835	18.555	19.095
	80%	14.38	19.885	7.99
500	10%	21.06	20.53	11.875
	40%	19.16	18.46	16.79
	80%	22.56	19.81	11.415

communication link is expected between the measurement transformers or the electronic digital devices that will be installed at the line's ends. However, in case of failing the communication link between the devices at the line's ends a redundant communications path might be applied for maintaining availability of the proposed scheme. Otherwise, a directional comparison scheme combined with modified distance element mentioned in [10] might be the most appropriate option for the proposed algorithm backup.

2.3. *Effect of fault impedance*

From Fig.1(a), the line's voltage at local and remote ends can be estimated as follows:

$$V_A = I_A Z_S \tag{14}$$

$$V_A = V_f \frac{Z_S}{R_f + (Z_S + mZ_L) \parallel (Z_R + (1-m)Z_L)} \left(\frac{Z_R + (1-m)Z_L}{Z_S + Z_L + Z_R} \right) \tag{15}$$

$$V_B = I_B Z_R \tag{16}$$

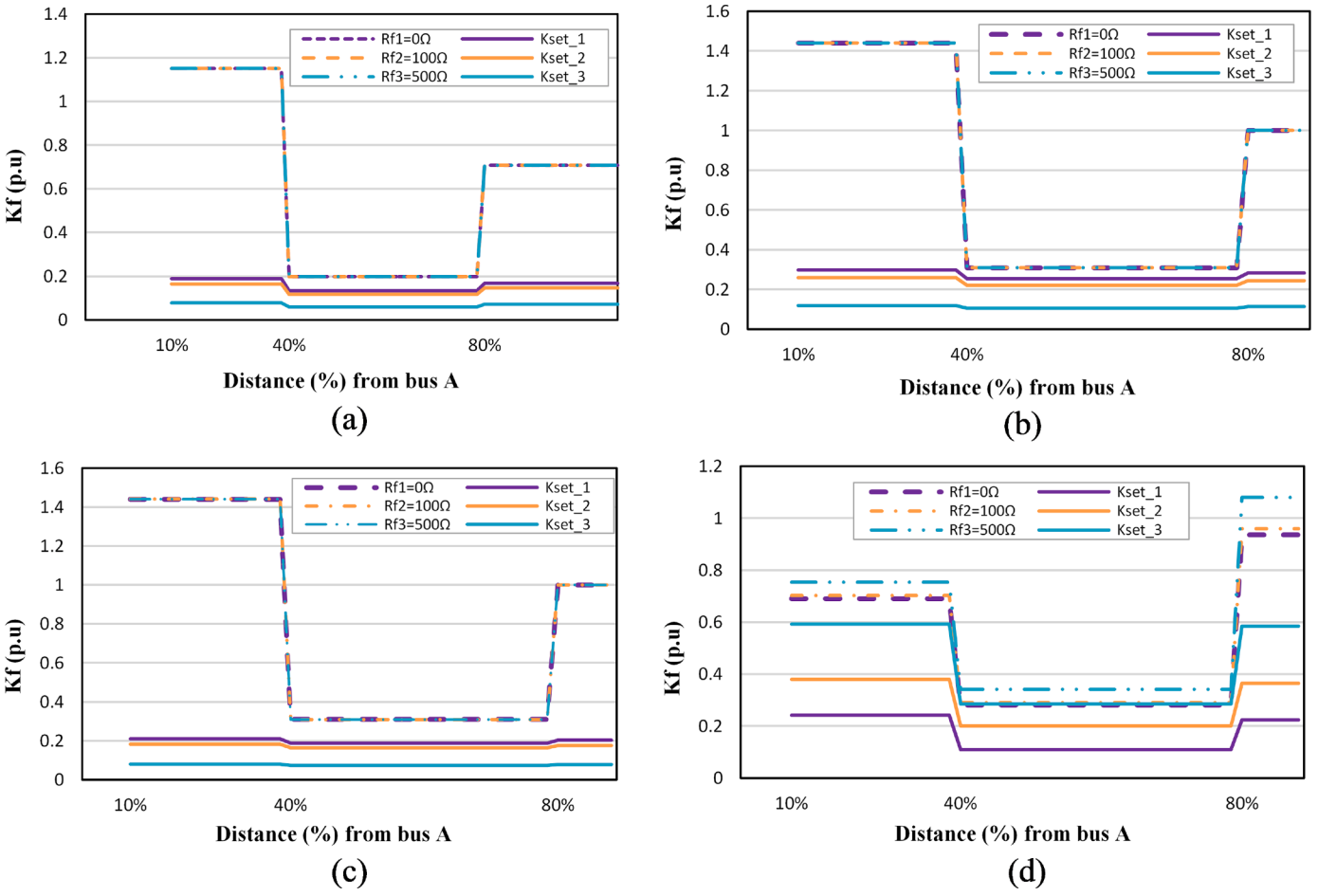

Fig. 5. Proposed protection algorithm behavior when only synchronous generator connected to the network during internal (a) SLG fault, (b) LL fault, (c) LLG fault, (d) LLLG fault

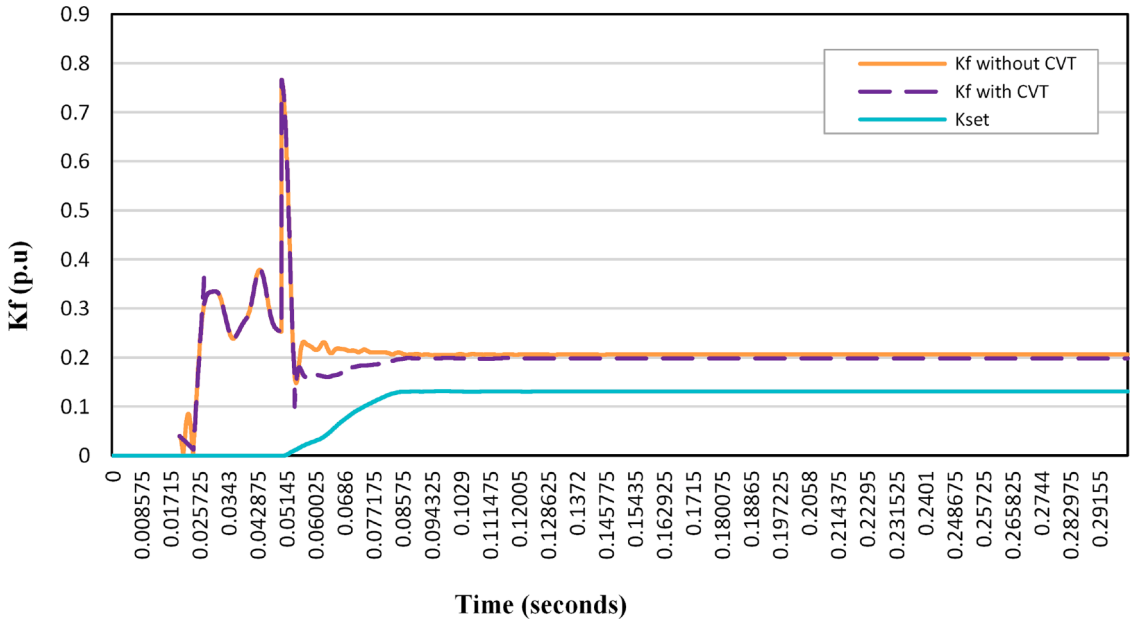

Fig. 6. Capacitive voltage transformer transient effect.

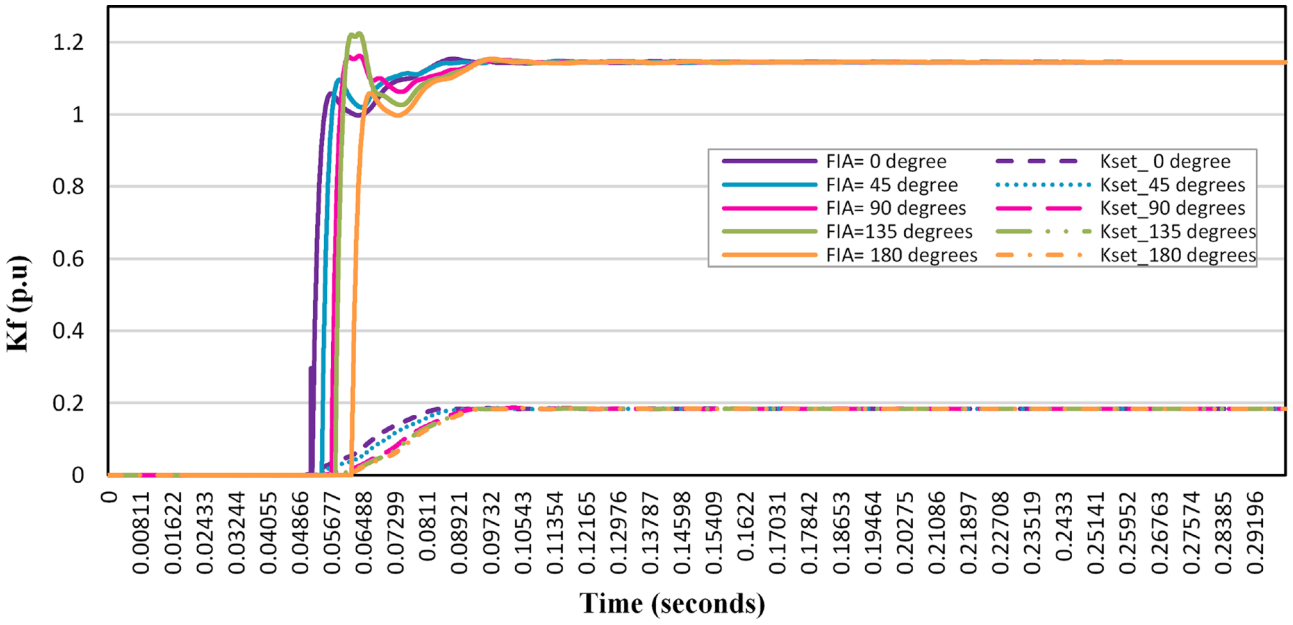

Fig. 7. Fault inception angle effect

$$V_B = V_f \frac{Z_R}{R_f + (Z_S + mZ_L) \parallel (Z_R + (1-m)Z_L)} \left(\frac{Z_S + mZ_L}{Z_S + Z_L + Z_R} \right) \tag{17}$$

$$K_f = \frac{|V_A - V_B|}{0.5(V_A + V_{B)}} = \frac{|Z_S(Z_R + (1-m)Z_L) \ - Z_R \ (Z_S + mZ_L)|}{0.5(Z_S(Z_R + (1-m)Z_L) + Z_R \ (Z_S + mZ_L))} \tag{18}$$

Eq. (18) shows that the fault indicator, K_f, is sovereign of fault resistance (R_f), hence, the proposed algorithm's sensitivity is not affected by R_f sequentially. Fig. 4 simulation results prove that K_f remains the same despite the fault resistance values when a fault occurs at the same position for all fault types shown in Fig 4. (a, b, c, and d) tested under different fault resistances ranged from 0, 100 and 500 Ω at 10 km, 200 km and 450 km from bus A and all faults are created at time = 0.05 second.

However, Table 1. showed that with a higher fault resistance value, more time requires the algorithm to trip. This is true for three reasons; first, when resistance increases, a sequential rise is expected in voltage component; second, due to the characteristics of the sequence voltage distribution when a fault occurs within the protected section of the line [16]. Finally, as per the fault indicator and threshold values are changing proportionally during internal faults.

Fig.4 (a) shows how K_{set} values are close to the K_f value during LG fault and this decrease when higher fault resistance is performed. Similar performance is noticed for other types of faults in Fig.4.

As with Fig. 4 results, shows a high performance of the proposed algorithm when no IBRs connected to the network. The algorithm operates within less than one cycle of fault occurrence time. Similar performance noticed under different fault events on different locations of the tested line Fig 5.

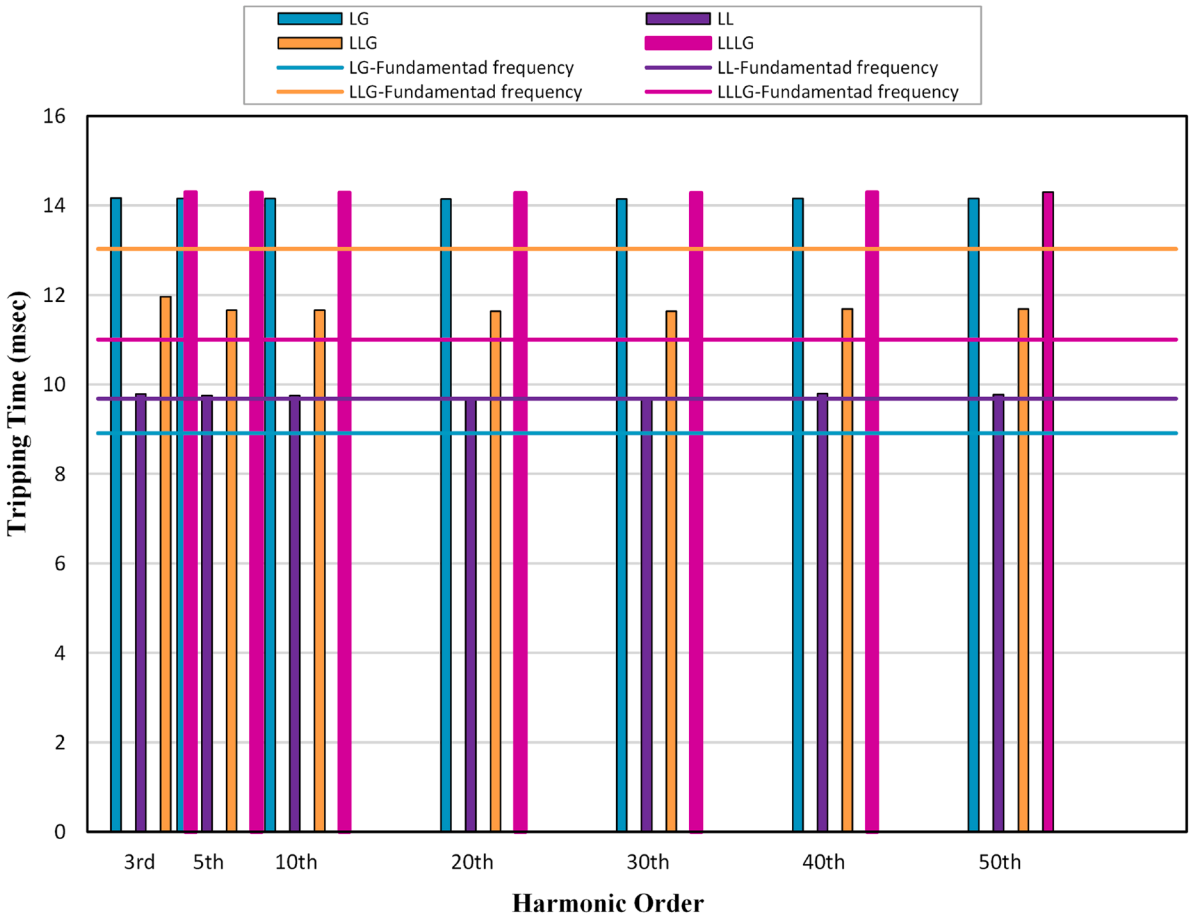

Fig. 8. Voltage harmonic impact on the proposed protection algorithm under different fault events

2.4. Effect of fault position

Fig.4 interpreted how the fault position affects the proposed algorithm's sensitivity, particularly when the fault location moves towards the middle of the line. According to Eq. (8), K_{set}, value is dependent on the maximum measured value of the voltage sequence component at the line's ends. Hence, the K_{set} modifies automatically to compile with the K_f value at each time. Hence, when the voltage component value goes down around the middle of the line, K_f decreases where Eq. (18) shows that K_f is dependent on the fault location (m). However, K_f still be higher than the setting value and the tripping time always within one cycle after fault occurrence, as shown in Table 1.

shows that the proposed algorithm operates reliably when only synchronous generator supplies the network. However, a longer tripping time has been noticed due to the dependency on voltage components rather than the current ones. Current sequence components are higher in magnitude than the voltage sequence components when fewer power electronic elements-based resources connected to the networkTable 2.

2.5. Effect of measurement instruments

Due to the low fault current from IBR, the current transformer challenging performance is avoidable when compared to its behavior with conventional synchronous sources [3]. Capacitive voltage transformer impact on the proposed algorithm has been studied and its transient effect is modeled based on [17, 18]. shows the algorithm operation when a ground fault is performed at time =0.05 second with and without voltage transformer transient effect. An insignificant impact is noticed between both operations, concluding that the algorithm can perform accurately under capacitive voltage transformer abnormal operation Fig. 6.

2.6. Effect of Fault inception angle

The fault inception angle (FIA) has been investigated for a SLG fault at 10% distance from bus A. The fault created at different FIAs (0°° 45°°, 90°°, 135°°, 180°°), i.e. When voltage is at different values for the faulted phase, which is phase A in this case. shows that the proposed identification factor K_f tested successfully to be higher than K_{set} in all tested scenarios Fig. 7.

2.7. Voltage harmonic impact

In the proposed algorithm, power electronics, inverters, are utilized on one side of the utility transformers to actively isolate voltage harmonics at the point of common coupling and regulating the load voltage at the same time. However, the proposed algorithm has been tested under voltage harmonic distortion to verify the algorithm reliability under faulty events. The test has been done by injecting voltage harmonics of orders up to 50th to investigate the impact of voltage harmonics on the proposed protection algorithm. All fault types have been performed at 10% distance from bus A. the faults have been simulated at the 3rd, 5th, 10th, 20th, 30th, 40th and 50th voltage harmonic. By comparing the algorithm tripping time under those scenarios with a similar event under the fundamental frequency, it has been observed that this algorithm operates reliably under harmonic distortion impact. Although, when LLG faults took place faster tripping time is noticed comparing to the fundamental frequency scenario however the time difference is very small, a 1.6 msec that can be ignored as long as the algorithm can detect the fault and operate in less than one cycle time as

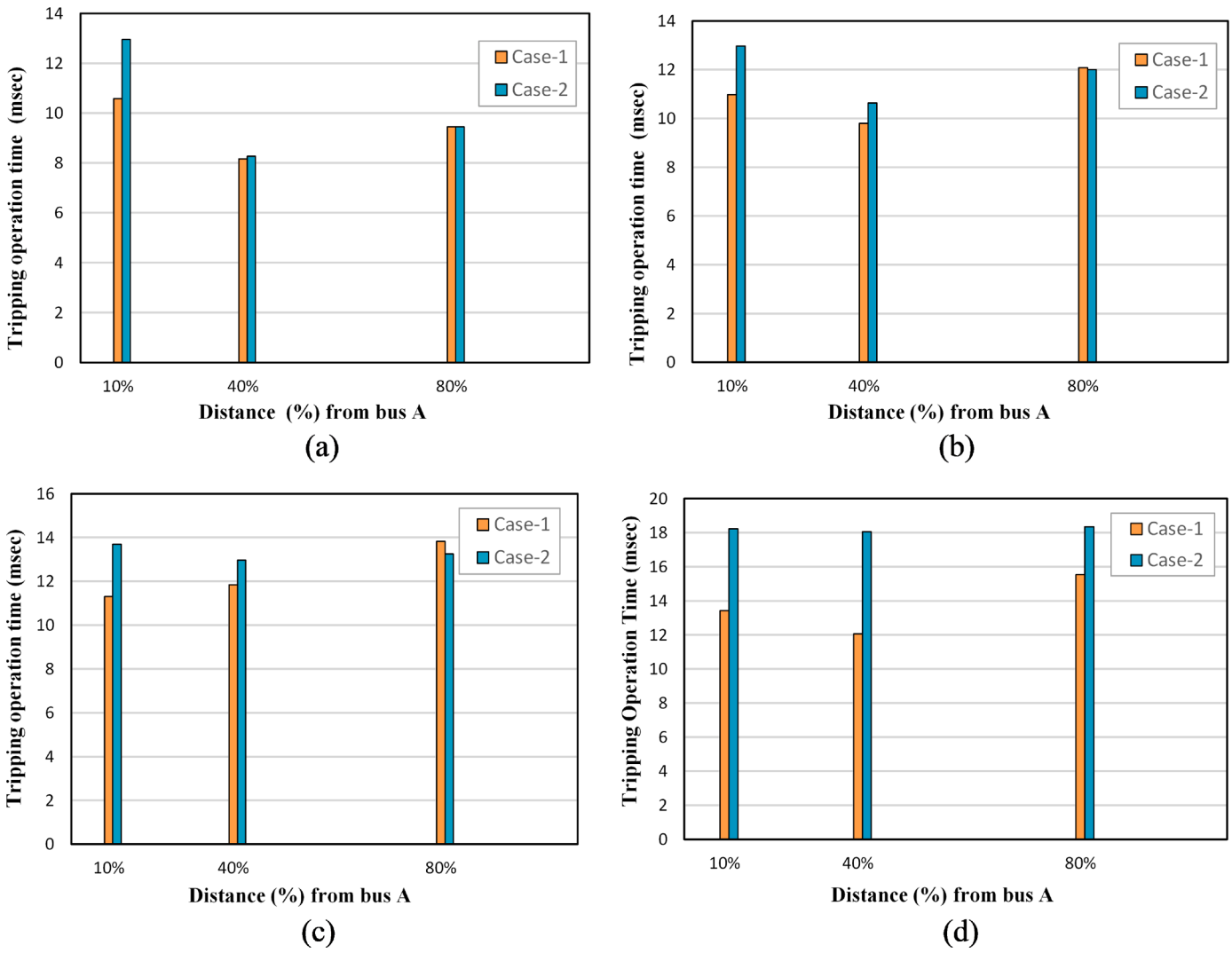

Fig. 9. Control Strategy impact on the proposed algorithm during internal (a) SLG fault, (b) LL fault, (c) LLG fault, (d) LLLG fault.

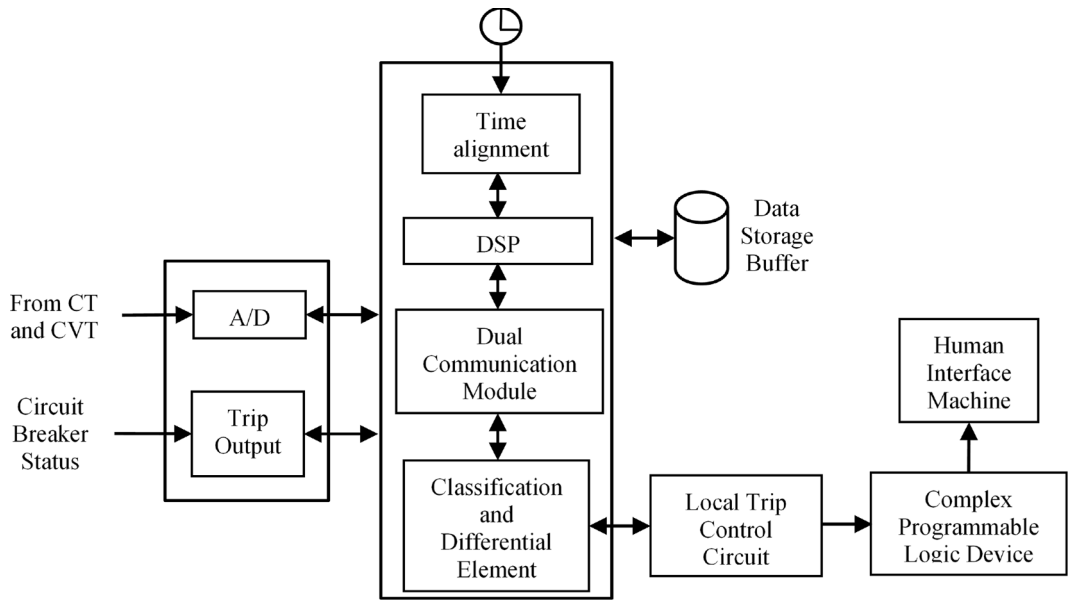

Fig. 10. Block diagram of the proposed relay

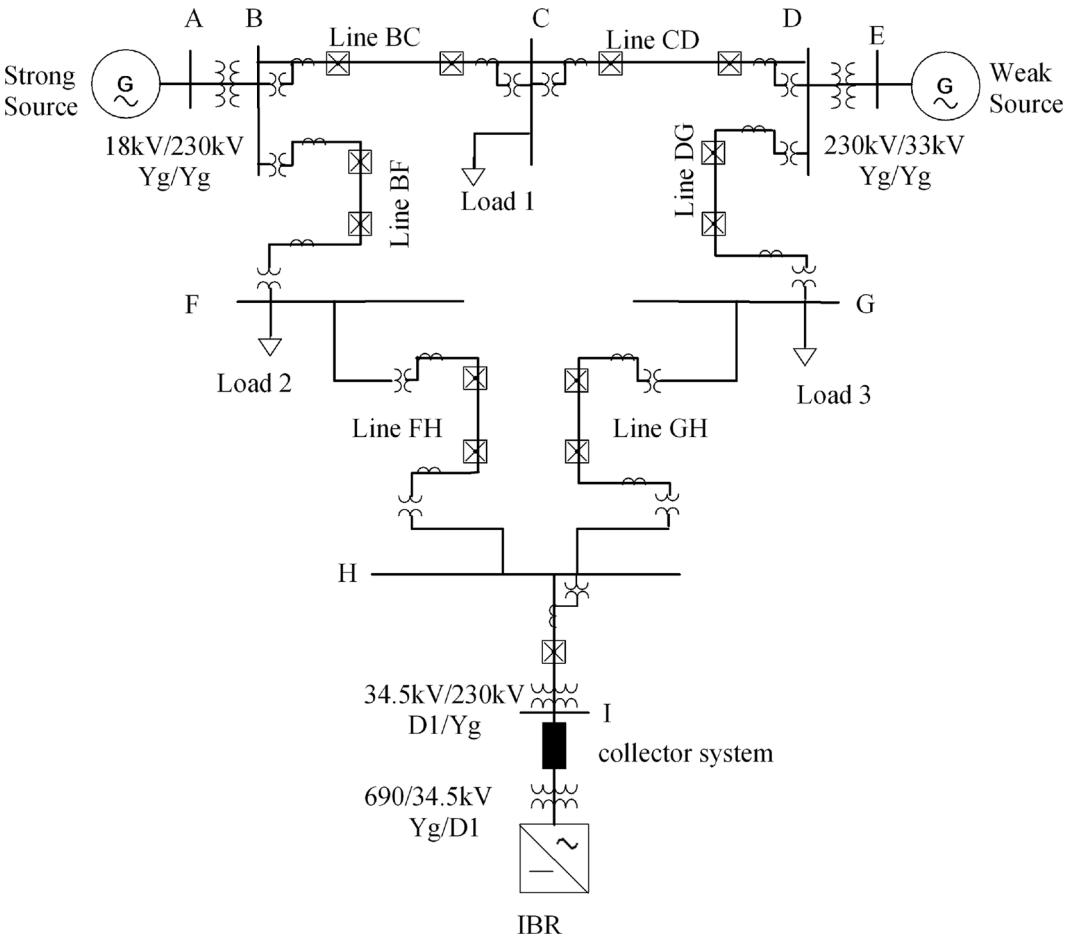

Fig. 11. Schematic diagram of IEEE-9bus study system for the proposed algorithm performance

shown in. Hence, it can be concluded that this algorithm can detect faults and operate reliably in the presence of harmonic distortion Fig. 8.

2.8. Impact of IBR's control strategies on the proposed algorithm

This paper investigation based on the type IV wind turbine generator with full scale convertor model detailed in [19] alongside its control strategies. The Fig. 2 network tested when the short circuit event is fully provided by the wind plant and its full-scale converter to investigate the plant's control strategies impact on the proposed algorithm, the current control and fault ride through control strategies have been also considered under case study-1. By comparing the results to case study-2, where constant active and reactive power control have been applied, a slight difference in tripping operation time has been noticed ensuring that the control strategy has a small impact on the proposed algorithm when tested under different fault types and locations. shows the simulation results comparison of cases1 and 2, it seems that a 2-4 msec difference in algorithm response time when between case-1 and 2. This difference can be seen clearly when symmetrical faullt took place in comparison to the other fault types applied. However, the algorithm response still considered reliable as it operated within less than one cycle time Fig. 9.

3. Proposed relay hardware

The proposed scheme hardware implementation compromises the following as shown in below:

- Measurement circuits to collect the required measured electrical quantities
- Global positioning system (GPS) to align the incoming messages and modify the magnitudes received from the measuring circuits to conform a time reference.
- Digital signal processor (DSP)
- Data storage buffer which includes the instruction to be executed by the differential element. Instructions comprises the automatically and determined threshold and setting values such as the fault classification setting K_{com} and the threshold value K_{set} alongside aligning the incoming messages.
- Dual communication module between DSP and the differential element microprocessor
- Local trip control circuit to send the trip signal to the circuit breaker.
- Communication between devices would be through any type of communication links.

The relay receives data during all the different operation status, normal and abnormal conditions storing, displaying or recording the required information at the end user side, HIM Fig. 10.

4. Proposed algorithm application under different contingency events

To validate the proposed protection algorithm in a bigger power system network, a typical IEEE 9-bus, 230 kV transmission line system has been performed on MATLAB/SIMULINK. The network shown in is of 50 Hz frequency with a negligible number of high-frequency harmonics. However, the line's frequency-dependent parameters' characteristics

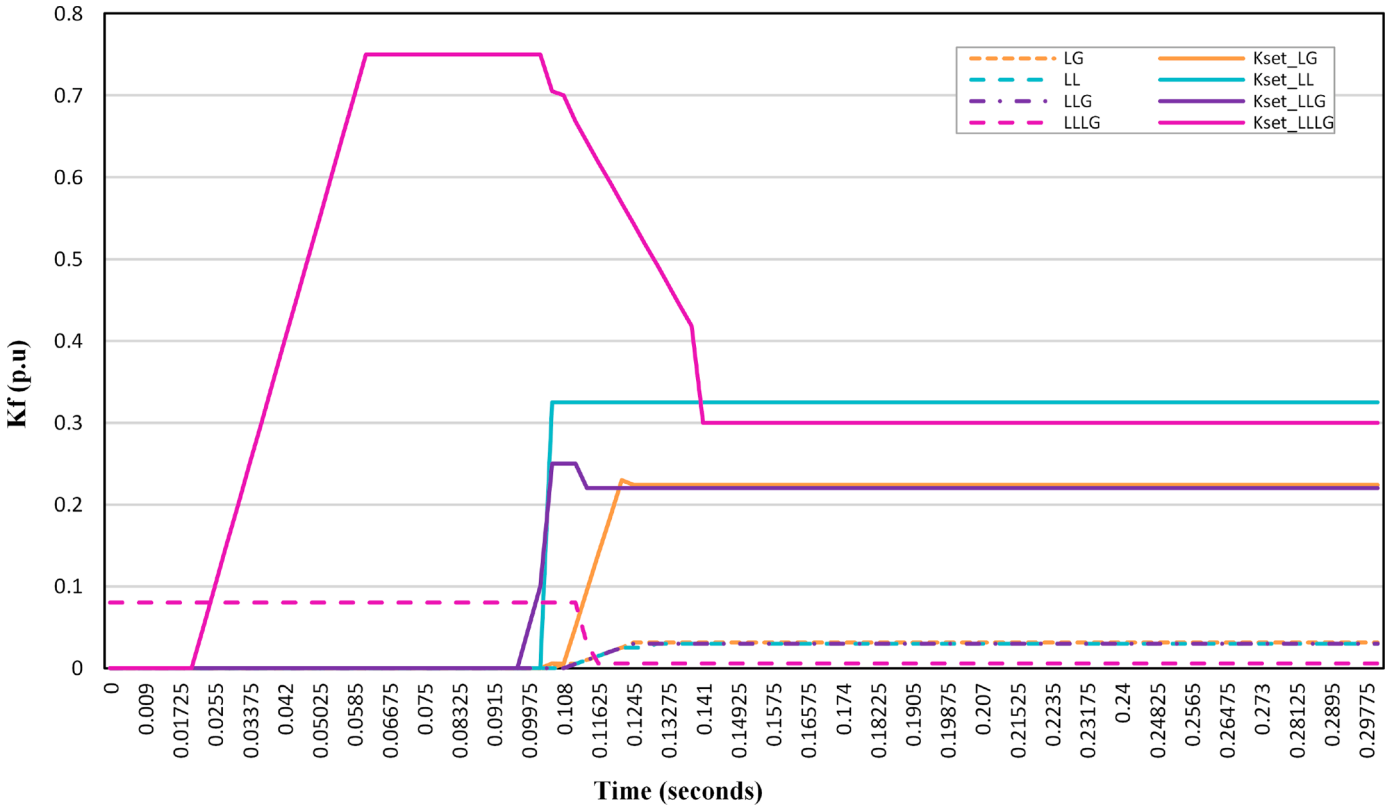

Fig. 12. Fault indicator and setting behaviour during External fault Between bus A and bus B

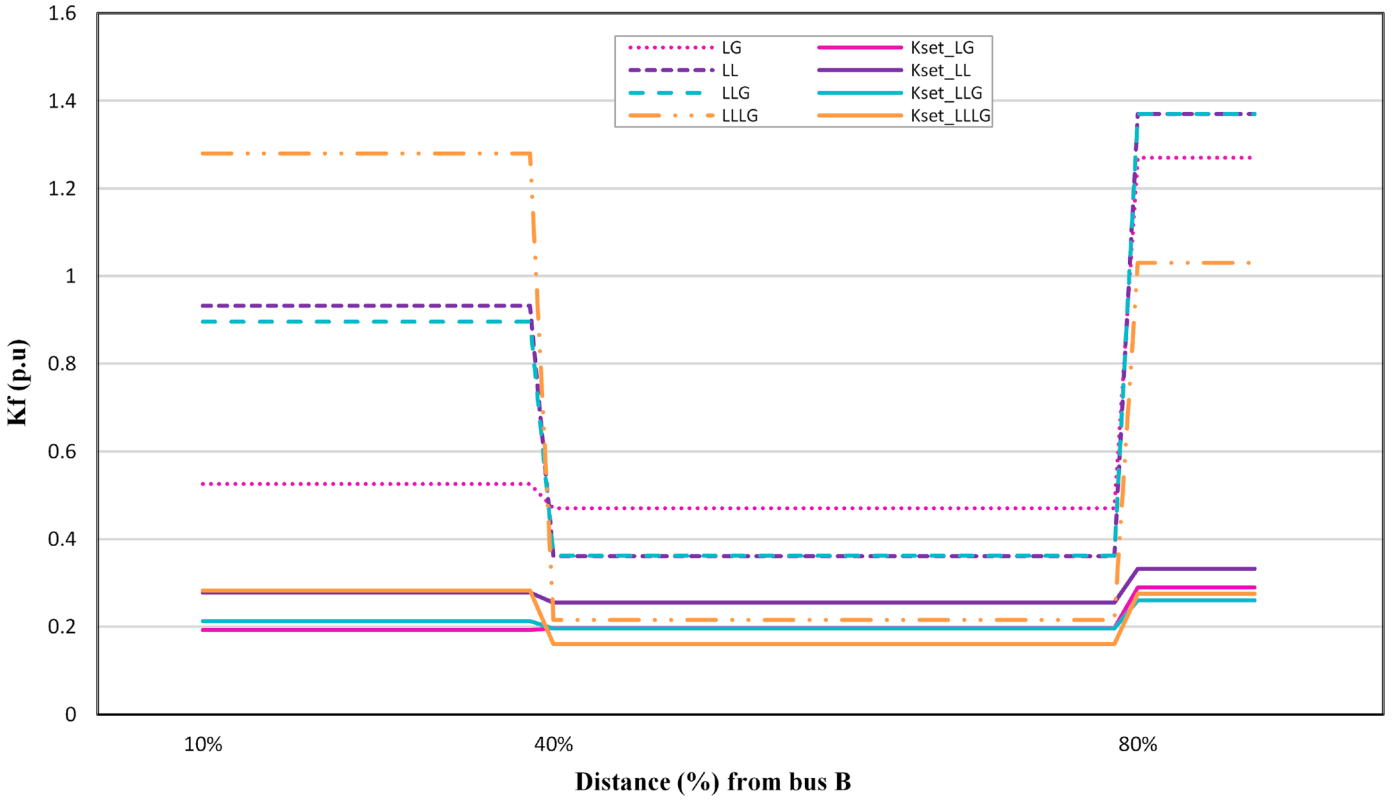

Fig. 13. Fault indicator and setting behaviour during internal (a) SLG fault, (b) LL fault, (c) LLG fault, (d) LLLG fault

Table 3.
Proposed Algorithm Operation in IEEE 9-Bus Network

Contingency Plan No.	Internal Fault Location	Distance fromleft hand side bus (%)	Fault Type			
			LG	LL	LLG	LLLG
			Tripping/Operation Time(msec)			
1	Fault on the line BC with Line CD out of service	10%	9.97	10.715	13	15.91
		40%	14.36	13.52	14.936	10.97
		80%	18.2	16.92	18.32	12.6
2	Fault on the line BC with Line DG and GH out of service	10%	9.52	10	12.145	23.68
		40%	11.66	10.87	12.335	21.66
		80%	14.735	12.62	13.85	19.52
3	Fault on the line BC with Line BF and FH out of service	10%	9.575	10.2	12.32	22.645
		40%	11.11	10.69	12.2	20.47
		80%	14.365	12.5	13.774	18.82
4	Fault on the line BC with no outage on other lines	10%	9.435	16.255	18.77	16.87
		40%	11.62	16.76	19.025	15.53
		80%	14.91	19.48	20.96	14.325
5	Fault on the line CD with Line BC out of service	10%	12.255	10.3	12.345	22.855
		40%	9.5	8.35	9.705	2072
		80%	6.955	6.35	6.685	18.105
6	Fault on the line CD with Line DG and GH out of service	10%	11.92	10.22	11.94	22.96
		40%	8.765	7.96	9.055	20.486
		80%	7.285	7.066	7.5	20
7	Fault on the line DC with Line BF and FH out of service	10%	13.39	11.5	13.095	21.66
		40%	9.998	9.095	10.72	19.37
		80%	7.69	7.455	8	20.755
8	Fault on the line BF with Line BC and CD out of service	10%	8.705	13.985	15.44	13.955
		40%	12.805	12.785	14.135	13.785
		80%	14.81	10.315	12.125	14.92
9	Fault on the line BF with Line DH and HG out of service	10%	7.97	8.995	10.9	12.29
		40%	12.535	12.14	13.415	10.13
		80%	16.455	14.54	16.05	8.39
10	Fault on the line DG with Line BF and FH out of service	10%	6.615	6.51	6.865	15.625
		40%	8.625	8.11	9.11	17.65
		80%	12.655	10.85	12.8	20.1
11	Fault on the line DG with Line BC and CD out of service	10%	5.825	6.2	6.49	18.43
		40%	7.32	6.455	6.855	20.41
		80%	10.18	8.355	9.76	23.495
12	Fault on the line DG with no outage on other lines	10%	6.415	6.73	7.085	15.655
		40%	8.295	7.824	8.705	17.66
		80%	12.115	10.445	12.305	20.04

are considered in this study. A strong source is connected to the local side (A) of the network, a weaker source connected to the remote side of the network (E) and a wind farm of 100 mills at busbar (I) is connected. Three main transformers, three loads and six-line sections are included in this network. The rated parameters of this IEEE 9-bus network are listed in Appendix A.2. Current transformers are considered to act ideally due to the expected low fault current. The capacitive voltage transformers are assumed to work typically, and their effect is not considered in this simulation Fig.11.

A type IV wind turbine based on the model detailed in [19] has been used. This model is more satisfactory to identify issues and challenges associated with IBRs, particularly when a weak network is performed. The main reason for choosing this type of IBRs as a test example in this paper that it is designed to extract the maximum amount of power from the applied wind speed of 15m/s by reducing the mechanical stress on the turbine during the gusts of wind. The full-scale converter is utilized in this model, which is known for its fast control on the active and reactive current and accurate response. These considered a strength point to be considered when connecting IBRs to the gird and active and reactive support become a big issue to take care of it.

This model is designed to apply the required ride-through criterion to ensure that the wind turbine stays connected to the grid during abnormal events. These criteria are vulnerable under weak network conditions, where proposed voltage-based protection reliability is tested. The algorithm's setting of K^{+}_{com}, K^{-}_{com} and K^{0}_{com} are chosen to be 1.2, 0.1, 0.1 respectively. Simulation test has been done in two stages:

1) involved an accurate fault detection operation for a practical network with successful discrimination between internal and external faults is performed as shown in. These faults initiated at 30% distance from bus B at time =0.05 second. With fault resistance = 0Ω.
2) included an overall comprehensive test on high impedance fault effect with fault resistance of 0, 100 and 500Ω. All fault types (LG, LL, LLG and LLLG) have been tested at different distances from the local end of the faulty line. Twelve different contingency scenarios are shown in Fig. 6 and Table 2. Due to the existence of two different source strengths, the fault detection process expected to be affected. However, the proposed algorithm operates properly with a tripping time of less than one cycle to operate compared to the time required

by conventional relays, as mentioned in [3]. From, it can be seen a minute rise above the 0.02 second expected tripping time when a symmetrical fault occurs. This can be attributed to the presence of the weak infeed source and the disconnection of the wind plant from one side of the network. However, the algorithm operates reliably and tripped faster than the existing relaysFigs. 12 and 13Table 3.

It worth to mention that protection coordination study is important to evaluate the trip settings of any protection algorithm and ensure a reliable operation of the system. In the existing power network, protection relays installed upstream downward would be over current relay or distance relay followed by differential relay. However, with proposed network of 90% IBRs connected to the network conventional relays expected to maloperate. Hence, in Fig. 11 network the protection initiation assumed to start with the proposed differential based algorithm. The proposed scheme considers as unit protection which is defined to protect a specific dedicated area of the protected element, unlike the other schemes it isolates the minimum area of the faulted element in comparison. Voltage components setting and the time interval between the proposed scheme devices must be ensured to guarantee a successful and reliable operation.

Usually, unit protection needs no coordination with other relays downward, However, If the proposed scheme operation fails in terms of operation time exceeded the minimum coordinating time, typically 1-2 cycles, or communication link lost, the operation will move mostly to the backup protection of the modified zone 2 distance relay with a directional comparison relay proposed in [10].

5. Conclusion

In this paper, a novel differential protection-based voltage component is proposed. The fault detection parameter is determined by the ratio between the difference and summation of both ends voltages of the protected line. The setting value is highly dependent on the maximum measured voltage component, which increases the algorithm operation reliability. Comparing to the existing protection schemes used with IBRs, the proposed algorithm is:

- Simple in the application and no need for complex techniques to measure, extract or transforming electrical quantities.
- Low time required for decision making and hence more sensitive operation.
- Operated accurately under high impedance faults, capacitive voltage transformer transient and weak source infeed.
- Having a compatible threshold value makes it easier to set the relay's functionality synchronously without need calculating different settings suits different sources strength.

CRediT authorship contribution statement

Safa Kareem Al-sachit: Conceptualization, Methodology, Software, Validation, Formal analysis, Investigation, Resources, Writing – original draft, Writing – review & editing, Visualization. **Nirmal K.C Nair:** Conceptualization, Methodology, Writing – review & editing.

Declaration of Competing Interest

The authors declare that they have no known competing financial interests or personal relationships that could have appeared to influence the work reported in this paper.

Appendix

A.1. Simple transmission network of Fig. 2 elements rating

Table. A.1.

Table A.1
Line and System's Parameters of Figure 2 network

	Parameter	Value
Source A	Nominal voltage	13.8 kV
	Frequency	50 Hz
	Short circuit level	5290 MVA
	System impedance ratio (X/R)	10
Source B	Nominal voltage	33 kV
	Frequency	50 Hz
	Short circuit level	5290 MVA
	System impedance ratio (X/R)	10
Transmission Line	Length	500 km
	Positive sequence impedance	0.249+j0.42678252 (Ω/km)
	Positive sequence capacitance	8.46704 nF/km
	Zero sequence impedance	0.747+j1.280335 (Ω/km)
	Zero sequence capacitance	5.751 nF

A.2. IEEE 9-bus system's parameters rating

Table. A.1Table. A.2.

Table A.2
Lines and System's Parameters of Figure 6 IEEE 9-bus network

	Rating
Strong Source	5290 MVA 18 kV 50 Hz X/R=10
Weak Source	1763 MVA 33 kV 50 HZ X/R=10
IBR	250 MW wind Plant 34.5 kV 50 Hz
All lines	100 km
Load 1	100 MW 35 MVar
Load 2	125 MW 50 MVar
Load 3	90 MW 30 MVar

References

[1] N. Nimpitiwan, S. Member, G.T. Heydt, R. Ayyanar, Machine and Inverter Based Distributed Generators, Power 22 (1) (2007) 634–641.
[2] J.M. Carrasco, et al., Power-electronic systems for the grid integration of renewable energy sources: A survey, IEEE Trans. Ind. Electron. 53 (4) (2006) 1002–1016.
[3] R. Chowdhury, N. Fischer, Transmission Line Protection for Systems With Inverter-Based Resources – Part I: Problems, IEEE Trans. Power Deliv. (2020).
[4] IEEE-PES Technical Report, "Impact of Inverter Based Generation on Bulk Power System Dynamics and Short-Circuit Performance," no. 68, July 2018.
[5] M. Nagpal, C. Henville, Impact of Power-Electronic Sources on Transmission Line Ground Fault Protection, IEEE Trans. Power Deliv. 33 (1) (2018) 62–70. Feb.
[6] G. Feng, G. Zhe, S. Zhang, J. Zhang, J. Dou, Influence on transmission line relay protection under Dfig-based wind farm intergration, in: Proc. 5th IEEE Int. Conf. Electr. Util. Deregulation, Restruct. Power Technol. DRPT 2015, 2016, pp. 290–295.
[7] A. Hooshyar, M.A. Azzouz, E.F. El-Saadany, Distance Protection of Lines Emanating from Full-Scale Converter-Interfaced Renewable Energy Power Plants-Part I: Problem Statement, IEEE Trans. Power Deliv. 30 (4) (2015) 1770–1780.
[8] A. Haddadi, I. Kocar, J. Mahseredjian, U. Karaagac, E. Farantatos, Performance of phase comparison line protection under inverter-based resources and impact of the german grid code, IEEE Power Energy Soc. Gen. Meet. (2020) 0–4, vol. 2020-Augus.

[9] A. Hooshyar, M.A. Azzouz, E.F. El-Saadany, Distance protection of lines connected to induction generator-based wind farms during balanced faults, IEEE Trans. Sustain. Energy 5 (4) (2014) 1193–1203.
[10] R. Chowdhury, N. Fischer, Transmission Line Protection for Systems With Inverter-Based Resources - Part II: Solutions, IEEE Trans. Power Deliv. (2020).
[11] A.K. Pradhan, G. Joós, Adaptive distance relay setting for lines connecting wind farms, IEEE Trans. Energy Convers. 22 (1) (2007) 206–213.
[12] S. Chen, N. Tai, C. Fan, J. Liu, S. Hong, Adaptive distance protection for grounded fault of lines connected with doubly-fed induction generators, IET Gener. Transm. Distrib. 11 (6) (2017) 1513–1520.
[13] H. AL-NASSERI, M.A. Redfern, A New Voltage based Relay Scheme to Protect Micro-Grids dominated by Embedded Generation using Solid State Converters, 19th International Conference on Electricity Distribution (0723) (2007) 1–4.
[14] J. Ma, W. Ma, X. Wang, Z. Wang, A new adaptive voltage protection scheme for distribution network with distributed generations," Can, J. Electr. Comput. Eng. 36 (4) (2013) 142–151.
[15] Z. He, Z. Zhang, W. Chen, O.P. Malik, X. Yin, Wide-area backup protection algorithm based on fault component voltage distribution, IEEE Trans. Power Deliv. 26 (4) (2011) 2752–2760.
[16] Z. He, Z. Zhang, X. Yin, H. Wang, A novel algorithm of wide area backup protection based on fault component comparison, 2010 Int. Conf. Power Syst. Technol. Technol. Innov. Mak. Power Grid Smarter, POWERCON2010 (2010) 1–7.
[17] D. Hou, J. Roberts, Capacitive voltage transformer: transient overreach concerns and solutions for distance relaying, Can. Conf. Electr. Comput. Eng. 1 (1996) 119–125. May 1996.
[18] R.L. De Andrade Reis, W.L.A. Neves, F.V. Lopes, D. Fernandes, Coupling Capacitor Voltage Transformers Models and Impacts on Electric Power Systems: A Review, IEEE Trans. Power Deliv. 34 (5) (2019) 1874–1884.
[19] A.S. Trevisan, A.A. El-Deib, R. Gagnon, J. Mahseredjian, M. Fecteau, Field Validated Generic EMT-Type Model of a Full Converter Wind Turbine Based on a Gearless Externally Excited Synchronous Generator, IEEE Trans. Power Deliv. 33 (5) (Oct. 2018) 2284–2293.